Journal of Experimental Botany, Vol. 64, No. 10, pp. 3061–3075, 2013
doi:10.1093/jxb/ert151 Advance Access publication 12 June, 2013

Journal of Experimental Botany
www.jxb.oxfordjournals.org

RESEARCH PAPER

Novel features of *Brassica napus* embryogenic microspores revealed by high pressure freezing and freeze substitution: evidence for massive autophagy and excretion-based cytoplasmic cleaning

Patricia Corral-Martínez, Verónica Parra-Vega and Jose M. Seguí-Simarro*

COMAV-Universitat Politècnica de València, CPI, Edificio 8E, Escalera I, Camino de Vera, s/n, 46022, Valencia, Spain

* To whom correspondence should be addressed. E-mail: seguisim@btc.upv.es

Received 18 February 2013; Revised 24 April 2013; Accepted 30 April 2013

Abstract

Induction of embryogenesis from isolated microspore cultures is a complex experimental system where microspores undergo dramatic changes in developmental fate. After ~40 years of application of electron microscopy to the study of the ultrastructural changes undergone by the induced microspore, there is still room for new discoveries. In this work, high pressure freezing and freeze substitution (HPF/FS), the best procedures known to date for ultrastructural preservation, were used to process *Brassica napus* microspore cultures covering all the stages of microspore embryogenesis. Analysis of these cultures by electron microscopy revealed massive processes of autophagy exclusively in embryogenic microspores, but not in other microspore-derived structures also present in cultures. However, a significant part of the autophagosomal cargo was not recycled. Instead, it was transported out of the cell, producing numerous deposits of extracytoplasmic fibrillar and membranous material. It was shown that commitment of microspores to embryogenesis is associated with both massive autophagy and excretion of the removed material. It is hypothesized that autophagy would be related to the need for a profound cytoplasmic cleaning, and excretion would be a mechanism to avoid excessive growth of the vacuolar system. Together, the results also demonstrate that the application of HPF/FS to the study of the androgenic switch is the best option currently available to identify the complex and dramatic ultrastructural changes undergone by the induced microspore. In addition, they provide significant insights to understand the cellular basis of induction of microspore embryogenesis, and open a new door for the investigation of this intriguing developmental pathway.

Key words: Androgenesis, cryomethods, doubled haploids, electron microscopy, haploids, microspore embryogenesis, rapeseed, ultrastructure.

Introduction

Microspore embryogenesis is a complex experimental process whereby a haploid microspore is reprogrammed to become a haploid or doubled haploid (DH) embryo. DHs are valuable tools for genetic and developmental research, but their principal application relates to plant breeding, where they may serve as pure lines for hybrid seed production. This androgenic switch is induced *in vitro* by the application of different types of abiotic stresses, including heat shock, cold, and starvation, among others (Shariatpanahi *et al.*, 2006). Therefore, the embryogenic microspore is an extremely complex *in vitro* biological system where cellular responses to abiotic stresses co-exist with the reprogramming towards a new developmental fate and the cessation of the old programme. It is easy to conceive that all these simultaneous changes must be reflected in a dramatic remodelling of cell architecture. Indeed, this topic has attracted the attention of cell biologists

since the discovery of this experimental phenomenon. As early as in 1974 Sunderland and Dunwell initiated the publication of their pioneering transmission electron microscopy (TEM) studies on the ultrastructural changes undergone by embryogenic microspores of *Nicotiana tabacum* (Dunwell and Sunderland, 1974*a*, *b*, 1975; Sunderland and Dunwell, 1974) and *Datura innoxia* (Dunwell and Sunderland, 1976*a*, *b*, *c*). Then, the identification of *Brassica napus* as a highly responding model system extended ultrastructural research to this species (Zaki and Dickinson, 1990, 1991; Hause *et al.*, 1992; Telmer *et al.*, 1993, 1995; Simmonds and Keller, 1999; Testillano *et al.*, 2000; Seguí-Simarro *et al.*, 2003, among others). For example, it was found that embryogenesis induction gives rise to a profound cytoplasm remodelling, including the clearing of large cytoplasmic regions devoid of organelles and ribosomes, the synthesis of different types of heat shock proteins, or the occurrence of somatic-type cytokinesis producing two equivalent nuclei and cells, as opposed to the asymmetric pollen mitosis where two clearly different generative and vegetative cells are formed. This approach continued providing useful insights in these and other species (for reviews, see Kasha, 2005; Maraschin *et al.*, 2005; Pauls *et al.*, 2006; Seguí-Simarro and Nuez, 2008*a*, *b*; Dunwell, 2010; Seguí-Simarro, 2010; Germanà, 2011), for a total of nearly 40 years of application of TEM to the study of microspore embryogenesis.

All the studies mentioned above had in common the use of the most popular procedures available at that time to preserve cell ultrastructure. In other words, they used aldehyde-based chemical fixatives (principally paraformaldehyde and glutaraldehyde) to preserve cells prior to TEM observation. These multifunctional fixatives are widely used, due principally to their relatively low cost, availability, and ease of use. They preserve cell ultrastructure by cross-linking subsets of cellular molecules, thereby preserving their spatial organization. However, it is important to note that chemical fixation takes seconds to minutes to immobilize cellular processes, and different cellular components are fixed at different rates (reviewed in Gilkey and Staehelin, 1986). Considering that subcellular elements such as phragmoplasts comprising microtubules and microfilaments, growing cell plates, vacuolar systems, Golgi stacks, or secretory vesicles undergo structural changes in the time range of seconds and even fractions of seconds, it is easy to deduce that most short-lived structural intermediates, in particular those of a membranous nature, will be created and dismantled before chemical fixatives have enough time to fix them. Further, penetration of chemical fixatives imposes on cells severe osmotic stresses known to cause swelling or shrinkage of cells and organelles, whose main ultrastructural consequence is the presence of wavy membrane contours (Lee *et al.*, 1982). In addition to this, it is well known that glutaraldehyde may cause vesiculation of the endoplasmic reticulum (ER), plasma membrane, or chloroplast membranes, and, in parallel, artefactual fusion of vesicles with the plasma membrane (Gilkey and Staehelin, 1986). In other words, chemical fixatives may potentially create artefactual vesicles in regions where they should be absent, or eliminate them from regions where they are actually present. Since these subcellular elements are below the resolution of conventional light and confocal microscopes, their deleterious effects are not detected with these microscopic approaches. However, all of these facts count against the notion of chemical fixatives as ideal tools for preserving cell ultrastucture to be observed by TEM.

Today, chemical fixation methods are being progressively replaced by ultrarapid, low temperature-based fixation technologies. Among them, the combination of high pressure freezing (HPF) with freeze substitution (FS) is nowadays the best option to avoid the limitations of chemical fixatives. HPF has the potential to stabilize the cells instantly, due to its ability to immobilize all cellular molecules within milliseconds (Gilkey and Staehelin, 1986). Samples preserved in this manner can then be freeze-substituted at –80 °C to –90 °C, which increases the probability of viewing even the most labile cellular structures. HPF/FS presents only one disadvantage for routine use: its high cost and therefore its reduced availability. Perhaps this is one of the reasons why these methodologies have not been used to study the changes undergone by microspores as a consequence of induction of embryogenesis.

In this work, HPF/FS was applied to process samples of *B. napus* isolated microspore cultures at different stages before, during, and after induction of embryogenesis. We revisited the ultrastructural changes undergone by the different cell types present in cultures, comparing them with other *in vivo* and *in vitro* microspore-derived structures. Thanks to the application of this improved methodology, we were able not only to confirm previous observations, but also to discover new subcellular structures involved in processes considered critical for a successful switch.

Materials and methods

Plant materials

Brassica napus L. donor plants of the highly embryogenic cv. Topas were grown as previously described (Seguí-Simarro *et al.*, 2003). Plants were grown in the greenhouses of the COMAV Institute (Universitat Politècnica de València, Valencia, Spain), the University of Colorado (Boulder, CO, USA), and Plant Research International (Wageningen, The Netherlands), at 20 °C under natural light.

Brassica napus microspore culture

Flower buds containing mostly vacuolated microspores were selected as previously described (Seguí-Simarro *et al.*, 2003), surface sterilized with 5.25 g l^{-1} sodium hypochlorite for 5 min, and washed three times in sterile distilled water. To release the microspores, buds were gently crushed in filter-sterilized NLN-13 medium with the back of the plunger of a disposable 50 ml syringe. NLN-13 medium (Lichter, 1982) consists of NLN medium+13% sucrose. Then, the slurry was filtered through 41 µm nylon cloths. The filtrate was transferred to 50 ml conical tubes and centrifuged at 800 rpm for 3 min. After discarding the supernatant, the pellet of microspores was resuspended in 10 ml of fresh NLN-13 medium. This procedure was repeated twice for a total of three centrifugations and resuspensions. Before the last centrifugation step, the microspore concentration was calculated using a haemacytometer. The required volume of NLN-13 medium was added to adjust the suspension to a concentration of 4×10^4 microspores ml^{-1}. The adjusted microspore suspension was distributed in sterile culture dishes. Dishes were incubated in

darkness for 24 h at 32 ºC to induce embryogenesis, and then continuously at 25 ºC for progression of embryogenesis. Culture dishes were checked on a daily basis under a inverted microscope. Dishes at different stages, as described below, were collected and processed by HPF/FS.

Processing of B. napus anthers and microspore cultures for transmission electron microscopy

For *B. napus* anthers, three batches were processed under the same conditions. Randomly selected anthers carrying microspores and pollen grains at different stages of microsporogenesis and microgametogenesis were excised from buds, immediately transferred to aluminium sample holders, cryoprotected with 150 mM sucrose, frozen in a Baltec HPM 010 high-pressure freezer (Technotrade, Manchester, NH, USA), and then transferred to liquid nitrogen. For *B. napus* microspore cultures, three independent cultures were performed over a period of 2 months. For each culture, 4-day-old microspore cultures were randomly selected and collected by gently spinning culture medium. Microspore-derived embryos (MDEs) at different stages were manually picked up from cultures at different days of culture. These samples were transferred to aluminium sample holders, cryoprotected in sucrose-rich NLN-13 culture medium, and frozen in a high-pressure freezer as described above.

Samples were then freeze substituted in a Leica AFS2 system (Leica Microsystems, Vienna, Austria) with 2% OsO_4 in anhydrous acetone at –80 ºC for 7 d, followed by slow warming to room temperature over a period of 2 d. After rinsing in several acetone washes, they were removed from the holders, incubated in propylene oxide for 30 min, rinsed again in acetone, and infiltrated with increasing concentrations of Epon resin (Ted Pella, Redding, CA, USA) in acetone according to the following schedule: 4 h in 5% resin, 4 h in 10% resin, 12 h in 25% resin, and 24 h in 50, 75, and 100% resin, respectively. Polymerization was performed at 60 ºC for 2 d in a vacuum oven. From the resin blocks obtained from each culture, a minimum of five were randomly selected and sectioned for further analysis. Using a Leica UC6 ultramicrotome, thin sections (1 µm) were obtained for light microscopy observation, and ultrathin sections (~80 nm) were obtained for electron microscopy. Ultrathin sections were mounted on formvar-coated copper, 200 mesh grids, stained with uranyl acetate and lead citrate, observed, and photographed in a Philips CM10 transmission electron microscope equipped with a Keenview Digital Camera (Soft Imaging System, Muenster, Germany). A total of 3158 digital micrographs were taken and analysed in this work.

Staining of B. napus microspore cultures with monodansylcadaverine and processing for confocal laser scanning microscopy

Samples of *B. napus* freshly isolated microspores and microspore cultures were collected immediately after isolation and at day 4 after induction, respectively. In addition, culture dishes containing MDEs at different developmental stages were picked up from cultures at different days of culture. Samples were fixed with 4% paraformaldehyde in phosphate-buffered saline (PBS) pH 7.4. Then, samples were placed on glass slides with 1.8% agarose, and stained with 10 µg ml^{-1} propidium iodide (PI) in PBS for 10 min. After three washes with PBS, samples were stained with 0.1 mM monodansylcadaverine (MDC; Sigma-Aldrich) for 10 min and washed again three times with PBS. Finally, slides were mounted with Vectashield mounting medium and observed with a Leica CTR 5500 confocal laser scanning microscope equipped with ×40 (NA 1.15) and ×63 (NA 1.30) oil-immersion lenses. For visualization of MDC, samples were excited at 405 nm and the emission window was set at 455–489 nm. For visualization of PI staining, samples were excited at 532 nm and the emission window was set at 583–703 nm. Digital images were processed with Leica Application Suite Advanced Fluorescence (LAS AF) software.

Results

Brassica napus isolated microspore cultures, including the freshly isolated microspores (Fig. 1A) just after isolation but before the application of the inductive treatment and the different structures produced after such a treatment, were processed by HPF/FS. Upon cessation of the inductive treatment, observation of microspore cultures revealed that they are heterogeneous systems where different types of structures typically co-exist. Although the first microspores showing external signs of change could be identified immediately after the end of the inductive treatment, the highest percentage (~40%) was observed at days 3–4 after induction. Apart from microspores which were arrested or dead (data not shown), 4-day-old cultures included pollen-like structures (Fig. 1B), derived from microspores that instead of entering embryogenesis followed a gametophytic-like pathway through which they enlarged, divided asymmetrically producing the generative and vegetative nuclei typical of pollen grains, and eventually arrested and died. Cultures also included microspores that divided symmetrically (Fig. 1C). For simplicity, these will be referred to hereinafter as embryogenic microspores, since daily observation of cultures revealed that they typically entered embryogenesis, producing suspensor-bearing, MDEs remarkably similar to their zygotic counterparts. In addition, cultures contained some microspores that underwent one or a few divisions, but did not follow either of the routes described above. Instead, the structures derived from these microspores used to be asymmetric, with enlarged cells of variable size (Fig. 1D). This feature made them easy to identify and follow during the different culture stages. Upon culture progression, these microspore-derived structures became arrested, not showing any sign of change or progression when observed at later stages. Eventually, they degenerated and died, never giving rise to MDEs. For this reason, they are referred to hereinafter as non-embryogenic structures.

Once processed by HPF/FS, the collection of TEM images covering all these structures was analysed, paying special attention to the ultrastructural differences between them. The results of this analysis are presented in the following sections.

Embryogenic microspores show specific ultrastructural features not present in other microspore-derived structures

Freshly isolated microspores at the optimal stage for induction (the vacuolated stage; Fig. 1A, A') presented a ribosome-rich cytoplasm, with abundant rough ER cisternae, and some Golgi stacks and mitochondria. The quality of the HPF/FS processing could be verified by the visibility of membranous elements such as Golgi cisternae, tonoplast, or plasma membranes (Fig. 1A'). These membranes presented smooth profiles, without the undulations typically present in many chemically fixed samples (Gilkey and Staehelin, 1986). Pollen-like structures (Fig. 1B), derived from microspores exposed to the same inductive conditions but not switching to embryogenesis, presented a dense cytoplasm, with abundant starch deposits and lipid bodies (Fig. 1B'). Mitochondria and

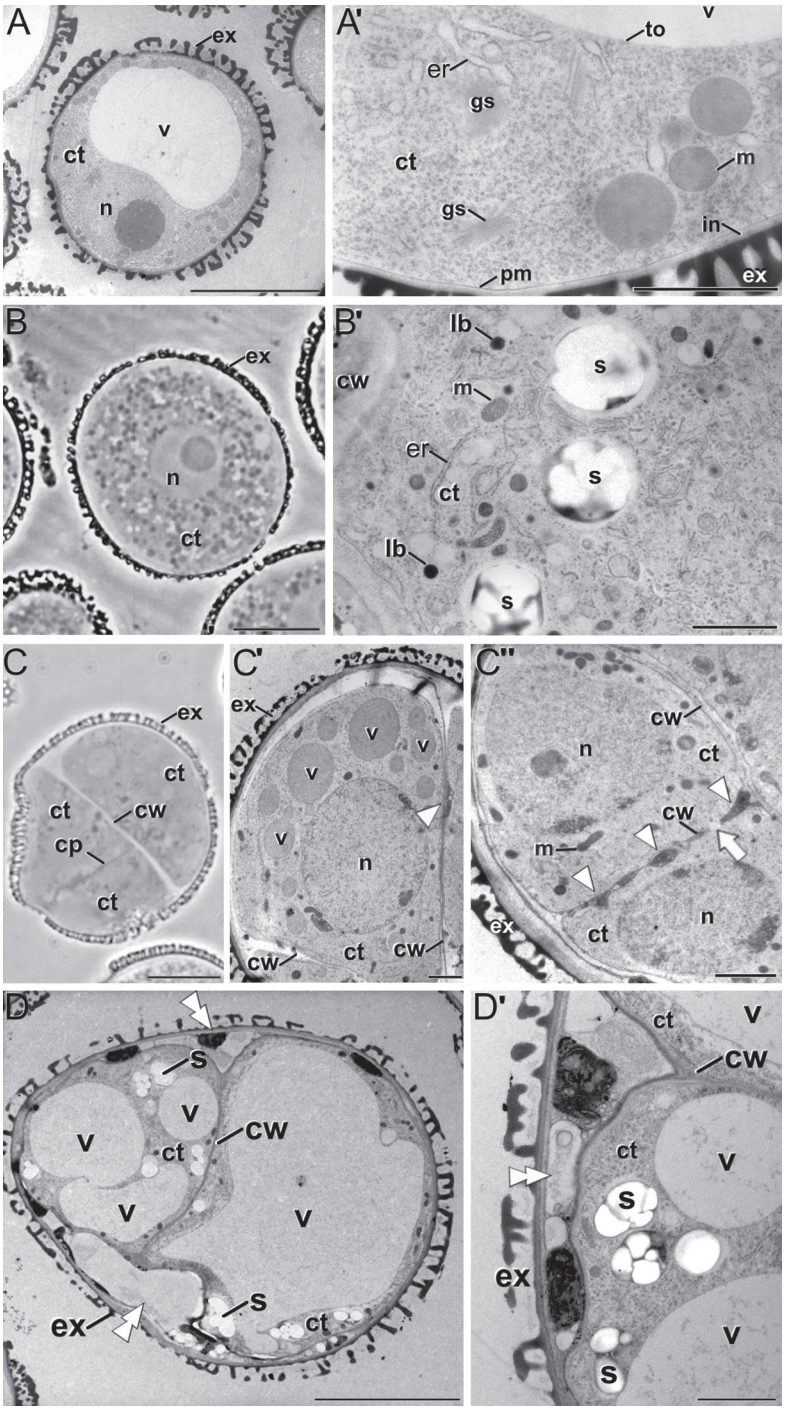

Fig. 1. Ultrastructure of *B. napus in vitro* cultured microspores. (A, A') Freshly isolated microspores, immediately before induction. (B, B') Pollen-like structure following a gametophytic-like developmental pathway. Note the presence of a dense cytoplasm (ct) with lipid bodies (lb) and large starch deposits (s) in amyloplasts. (C, C', C") Embryogenic microspores. Note the presence of several dense vacuoles (v), and of irregular cell walls (cw) with small fenestrae (arrow) and deposits of dense material (arrowheads). (D) Non-embryogenic structure. Note the massive vacuolation (v), the abundant starch deposits (s), and the presence of dead lateral cells (double arrowheads). (D') Detail of a non-embryogenic structure. Note the presence of necrotic remnants and cell debris in the dead lateral cell (double arrowhead). er, endoplasmic reticulum; ex, exine; gs, Golgi stack; in, intine; m, mitochondrion; n, nucleus; pm, plasma membrane; to, tonoplast. Bars: A–D, 10 μm; A'–D' and C", 2 μm.

long rough ER profiles were also characteristic of these cells, indicating a high biosynthetic activity.

In contrast, all the embryogenic microspores observed (Fig. 1C) presented a remarkably different ultrastructure. These two- to four-celled structures showed a cytoplasm with a considerably lower density of ribosomes, and some regions devoid of organelles. The nucleus was centrally positioned and surrounded by numerous, round, or slightly oval vacuoles of

up to 3 μm diameter (Fig. 1C'). These vacuoles, probably generated by fragmentation of the large vacuole of microspores, frequently presented electron-dense luminal contents, notably different from the light lumen of vacuolated microspores (Fig. 1A). Whereas mitochondria were present as in previous stages, starch deposits were almost absent, lipid bodies were scarce, and in general the cytoplasm was less densely filled than in other stages. Irregular cell walls and growing cell plates were observed, occasionally presenting holes and incomplete regions (arrow in Fig. 1C'') never observed in previous stages. However, the most striking feature of these cell walls was the presence of swollen and electron-dense regions (arrowheads in Figs. 1C', C''). In addition to this, unusual membranous profiles engulfing entire organelles and cytoplasmic regions were frequently observed in dividing cells (see next section). Once more, these profiles were absent from previous stages, and also from pollen-like structures.

Non-embryogenic structures usually presented a combination of some of the features described for pollen-like structures and embryogenic microspores. As seen in Fig. 1D, this type presented one or a few sporophytic divisions, as revealed by the presence of conventional cell walls, and abundant starch deposits, similar to those observed in pollen-like structures. Nevertheless, the most prominent trait of these cells was their enormous vacuolation. Vacuoles occupied most of the cellular volume, in the form of several vacuoles of different sizes, or of a single large, central vacuole. Accordingly, the cytoplasm was reduced to thin layers between vacuoles or between the vacuole and the plasma membrane. It was frequent to find some of their cells dying or dead, as revealed by the presence of necrotic remnants (Fig. 1D'). At later stages, this microspore-derived type, as well as pollen-like structures, always showed clear ultrastructural signs of general degeneration and death, indicating that they never proceeded further in embryogenesis, and eventually degraded and died (data not shown).

In summary, the ultrastructural analysis of the early stages of microspore embryogenesis revealed two main cell architectures: (i) that present only in embryogenic microspores, characterized by cell walls with swollen, electron-dense regions, and by membranous structures engulfing entire cytoplasmic regions; and (ii) that present in other microspore-derived types, not including any of these features, and never progressing through embryogenesis. Due to the significance of the features described for the embryogenic microspores, a detailed analysis of them was performed, as described below.

Embryogenic microspores present abundant autophagy-related elements

One of the principal features observed in embryogenic microspores was the presence of membranous elements engulfing large cytoplasmic regions (Fig. 2). Cup-shaped membranous elements, probably phagophores, were frequently observed (Fig. 2A), as well as closed, double membrane-bound elements enclosing small portions of cytoplasm (Fig. 2B), equivalent to those previously documented in autophagic processes and described as autophagosomes (Aubert *et al.*, 1996; Otegui *et al.*, 2005; Lundgren Rose *et al.*, 2006; Reyes *et al.*, 2011). Occasionally, phagophore-like structures (Fig. 2C) and autophagosomes (Fig. 2D) were observed enwrapping larger cytoplasmic domains containing different types of organelles. In addition to phagophores and autophagosomes, different types of vacuoles were observed with luminal contents of different levels of electron density (Figs. 2E–G), ranging from high, densely stained, to light. Light vacuoles used to present membranous remnants and masses of fibrillar material dispersed throughout the lumen. Sometimes vacuoles of different types were observed tightly apposed or in physical contact (Fig. 2G), suggesting fusion between them. Since these different vacuoles usually had a size similar to autophagosomes (0.5–3 μm), it was concluded that they could be representing different stages in the process of digestion of their contents. Larger autophagosomes were also observed, sometimes fusing with dark vacuoles (Fig. 2H), and also with large, light vacuoles derived from the fragmentation of the large vacuole of the original microspore (data not shown). Considering all these observations together, it is concluded that the structures observed corresponded to different steps of a typical process of macroautophagy, whereby cytoplasmic regions and even organelles were introduced into lytic vacuoles to be digested and recycled. Although sporadically, the presence of large (up to 5 μm) and complex membranous elements, either single- or double-membrane bound, with invaginations of their external membrane, similar to those described for microautophagic vacuoles (Fig. 2I), was also observed. These elements, similar to the pre-vacuolar compartments described in other plant systems (Reyes *et al.*, 2011), typically included small, single membrane-bound autophagic bodies, occasionally containing entire organelles. In contrast to embryogenic microspores, pollen-like structures (Fig. 1B, B') and non-embryogenic structures (Fig. 1D) did not show such a massive presence of autophagic profiles. Only scarce, isolated examples of such profiles could be sporadically identified in non-embryogenic microspores (data not shown). In summary, an abundant set of membranous elements was observed exclusively in embryogenic structures, that strongly pointed to the massive occurrence of macroautophagy, and, to a lower extent, microautophagy.

Embryogenic microspores undergo massive excretion of cytoplasmic material

In addition to the mentioned evidences of autophagy, the presence of abundant material unusually deposited in the cell walls of embryogenic microspores was observed (Fig. 3A). When observed at higher magnification, two types of material could be distinguished in cell walls. The first type presented a membranous nature (Fig. 3B). In general, these vesicle-like elements showed an enormous dispersion, with diameters ranging from 23 nm to 246 nm, and a majority ~30–40 nm (Supplementary Fig. S1A available at *JXB* online), indicating that they do not corresponded to conventional, Golgi-derived secretory vesicles (average diameter of 80–90 nm; Supplementary Fig. S1B). The second type was an electron-dense, homogeneously fibrillar material (asterisk in Fig. 3C),

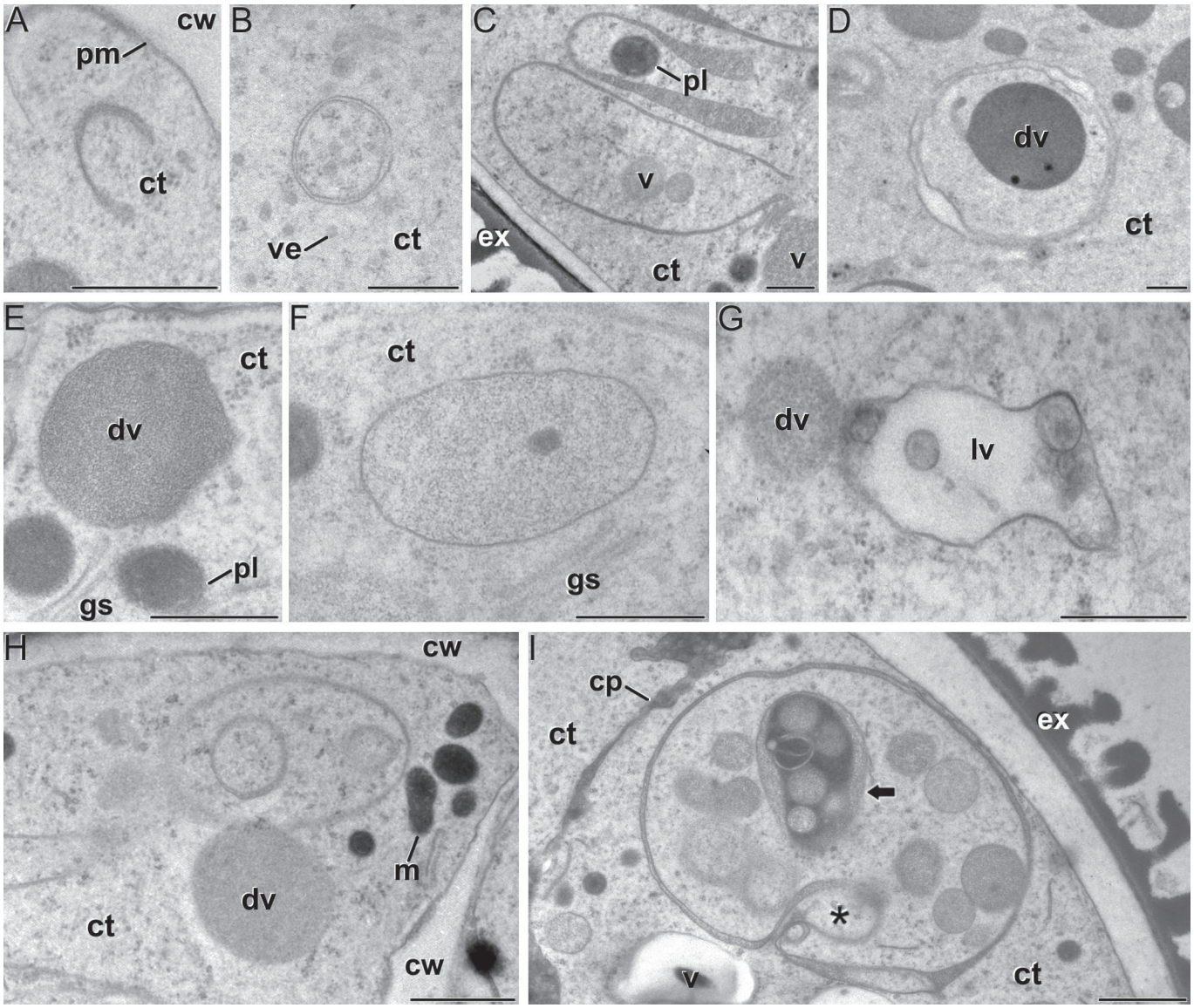

Fig. 2. Autophagy in embryogenic microspores. (A) Small phagophore. (B) Small autophagosome. (C) Large phagophore surrounding a small vacuole (v). (D) Large autophagosome containing a dense vacuole. (E–G) Dense (E), medium (F), and light (G) vacuoles, representing different stages during the digestion of their content. Note in G the close proximity of a dense vacuole (dv) and a light vacuole (lv), suggesting imminent fusion between them. (H) Large autophagosome contacting a dense vacuole (dv), suggesting fusion between them. (I) Large pre-vacuolar compartment containing autophagic bodies, one of them with an organelle, apparently a proplastid, being digested (arrow). Note the presence of an invagination (asterisk), suggesting a process of microautophagy. ct, cytoplasm; cw, cell wall; ex, exine; gs, Golgi stack; m, mitochondrion; pl, plastid; pm, plasma membrane; ve, vesicle. Bars: A–G, 500 nm; H and I, 1 μm.

identical to that observed in the lumen of dense cytoplasmic vacuoles (asterisks in Fig. 3A). As seen in Fig. 3A, dense cytoplasmic vacuoles were frequently observed in the vicinity of the cell wall. Interestingly, cell wall depositions were frequently observed at the side of the middle lamella corresponding to the cell with abundant dense vacuoles close to the cell wall (Fig. 3A). Very frequently, the extracellular fibrillar depositions (Fig. 3B) occupied an area equivalent to that of dense vacuoles (Fig. 3A). All these facts strongly suggested that the dense vacuoles and extracellular fibrillar depositions contained the same dense, fibrillar material. In other words, the observed profiles could be reasonably interpreted as if at least some of the dense vacuoles were directed to the plasma membrane, fused with it, and excreted their material to the cell wall. Occasionally, vacuoles containing a mixture of dense, fibrillar material and vesicle-like, membranous bodies were also observed (Fig. 3D). Consistent with the observations described for dense vacuoles and fibrillar deposits, extracellular deposits of fibrillo-vesicular material were also observed, with a size equivalent to that of fibrillo-vesicular vacuoles (Fig. 3E). Thus, it was deduced that the material illustrated in Fig. 3D and E was essentially the same, but observed at different moments during the process of excretion. Vacuoles containing membranous multilamellar structures fusing with the

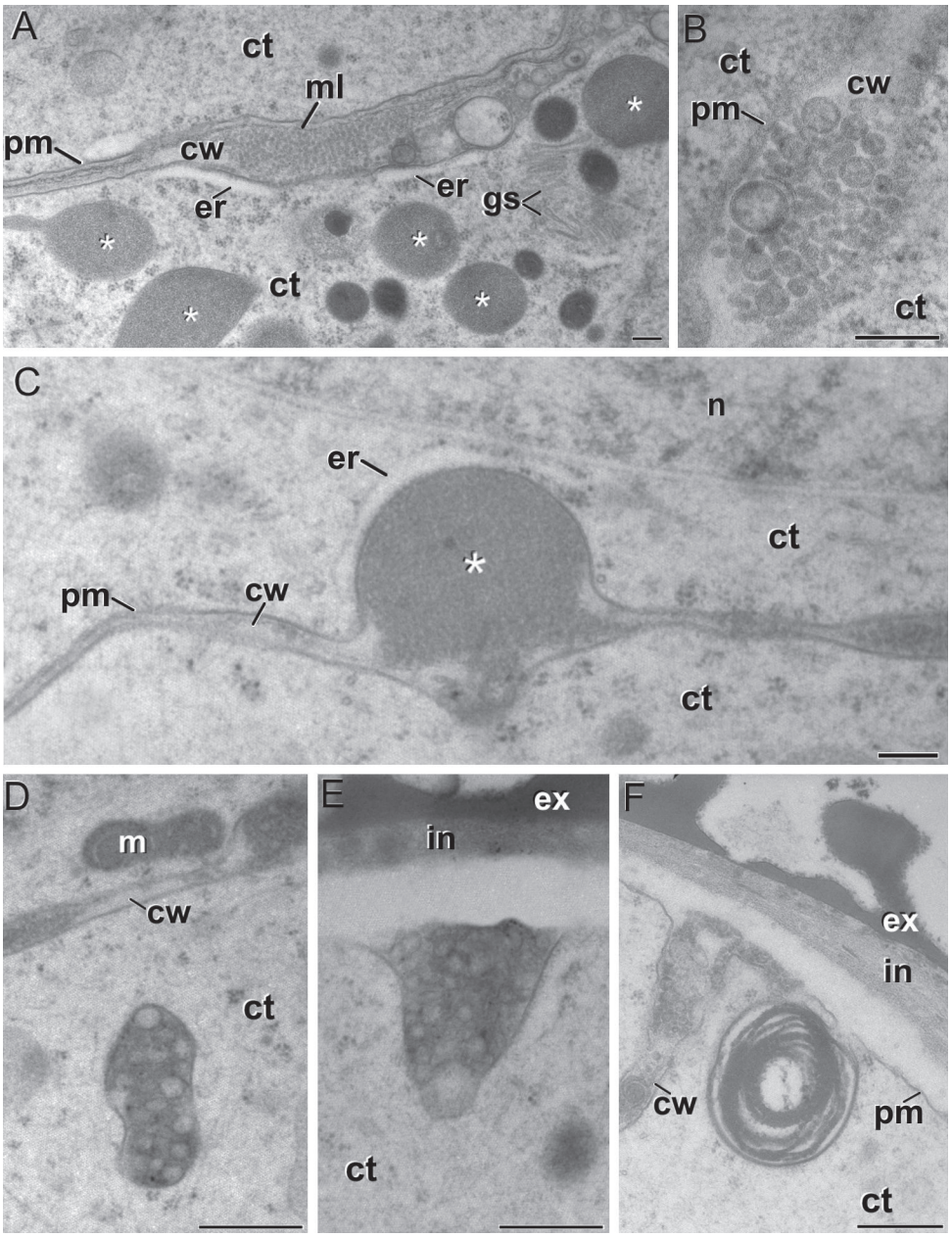

Fig. 3. Extracytoplasmic excretion in embryogenic microspores. (A) Newly formed cell wall (cw) with abundant vesicular material. Note that all the vesicles are at the side of the middle lamella (ml) where numerous dense vacuoles (asterisks) are observed close to the cell wall. (B) Enlarged view of a vesicular deposit, showing their membranous nature and their size heterogeneity. (C) Deposit of fibrillar, dense material (asterisk), similar in size to the dense vacuoles shown in A (asterisks). (D) Dense vacuole with fibrillo-vesicular material, near to the cell wall. (E) Fibrillo-vesicular cell wall deposit. Note the similarity between the deposited material and that of the vacuole shown in (D). (F) Multilamellar deposit fusing with the plasma membrane (pm). ct, cytoplasm; er, endoplasmic reticulum; ex, exine; gs, Golgi stack; in, intine; m, mitochondrion; n, nucleus. Bars: 200 nm.

plasma membrane were also identified (Fig. 3F). This material was remarkably similar to that previously described as remnants from the digestion of cytoplasmic organelles (Aubert *et al.*, 1996; Wu *et al.*, 2009). All the deposits described here were visible in newly formed cell walls (Fig. 3A–D), as well as in the microspore coat (Fig. 3E, F). In either case, the presence of these deposits was usually associated with swelling, irregularities, and in some cases dramatic deformations of the cell wall, most probably caused by the massive accumulation of this material. None of the structures described in this section was observed either in pollen-like structures (Figs. 1B, B') or in non-embryogenic structures (Fig. 1D).

In summary, several lines of ultrastructural evidence were identified which strongly suggested that embryogenic microspores (but not pollen-like or non-embryogenic structures) undergo a series of processes destined to excrete considerable amounts of intracellular, partially digested fibrillar and membranous material.

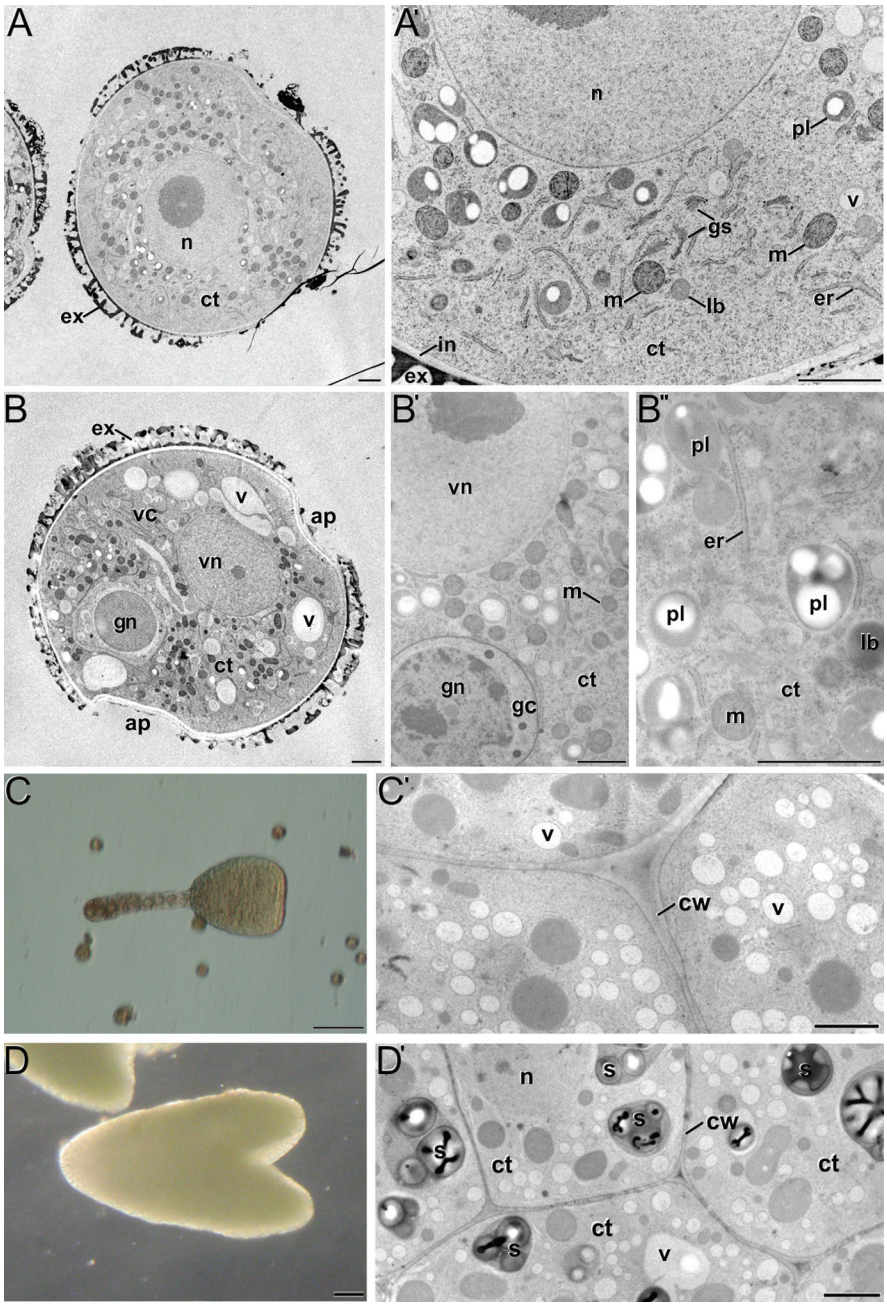

Fig. 4. Ultrastructure of *B. napus in vivo* nicrospores and pollen grains. (A) Overview of a young microspore within the anther. (A') Detail of the cytoplasm (ct) of a young microspore, showing a high ribosome density, abundant ER (er), Golgi stacks (gs), and to a lower extent, lipid bodies (lb) and small plastids (pl) beginning to accumulate starch. Very few, small vacuoles (v) are observed. (B) Overview of a bicellular pollen grain within the anther. Note the presence of several, medium-sized light vacuoles, probably produced from fragmentation of the large vacuole of the microspore. (B') Enlarged view showing the striking morphological differences between the vegetative (vn) and the generative nucleus (gn) of the generative cell (gc), embedded in the vegetative cell (vc). (B") Detail of the ribosome-rich cytoplasm of a vegetative cell, showing large starch-containing plastids (pl), mitochondria (m), and lipid bodies (lb). (C, C') MDE at the transition between globular and heart-shaped. A vacuolated cytoplasm, enriched in lipid bodies and with straight, conventional cell walls, can be seen. (D, D') Torpedo MDE, with the typical cytoplasm of *B. napus* embryo cells, characterized by massive accumulation of starch and lipid bodies. ap, aperture; ex, exine; in, intine; n, nucleus. Bars: 200 nm except for A, B (2 μm), and D, E (50 μm).

Young microspores, pollen grains, and MDEs do not show autophagic profiles or massive excretion

As an additional control to validate the unique ultrastructural features observed in embryogenic microspores, other stages during *in vivo B. napus* microsporogenesis and microgametogenesis, were processed by HPF/FS. Anthers containing young microspores, just released from the tetrad (Fig. 4A, A') and anthers containing bicellular pollen (Fig. 4B–B") were studied. These stages are before (microspores) and after (pollen) the developmental window when microspores are responsive to the

androgenic switch. Young microspores, prior to the formation of the large vacuole that displaces the nucleus close to the plasma membrane, presented a slightly lobed shape and a centred nucleus surrounded by organelles (Fig. 4A). The cytoplasm was dense, with abundant ribosomes, ER, Golgi stacks, mitochondria, and plastids initiating slight starch accumulation (Fig. 4A'). Only small, light vacuoles (up to 100 nm in diameter) were identified. No signs of autophagy were observed. The microspore coat consisted of a thin intine layer covered by a sculptured exine coat. No signs of any fibrillar or membranous deposit were observed in the coat of any of the microspores observed. Bicellular pollen grains presented the typical vegetative and generative cells, including their respective vegetative and generative nuclei (Fig. 4B). Whereas the vegetative nucleus was larger and presented a typical pattern of decondensed chromatin, the smaller generative nucleus showed a condensed chromatin pattern, with most chromatin masses close to the nuclear envelope (Fig. 4B'). The cytoplasm was densely filled with ribosomes, rough ER cisternae, lipid bodies, starch-containing plastids, and mitochondria (Fig. 4B''), typical of *B. napus* pollen grains. Only light vacuoles were observed, as expected for maturing pollen where the large microspore vacuole is fragmented and progressively reabsorbed. The pollen coat showed a thin intine layer, slightly thickened at the region of the apertures, and a more mature exine layer, with clear signs of pollenkitt deposition (Fig. 4B). Again, no indications of autophagy or massive excretion could be observed in these cells.

In vitro cultured, developing MDEs (Fig. 4C–D'), picked up between 6 d and 15 d after the end of the induction treatment, and covering the stages from globular to torpedo, were also processed and studied. In globular, transitional, and heart-shaped embryos (Fig. 4C), the unusual ultrastructural features described for embryogenic microspores were no longer observed. All cells presented smooth plasma membranes and straight cell walls with no gaps or dense deposits (Fig. 4C'). In other words, these cells presented conventional, somatic-type cell walls (Seguí-Simarro *et al.*, 2008), similar to their zygotic counterparts. The cytoplasm presented a conventional appearance as well. In torpedo MDEs (Fig. 4D), cells also showed the typical ultrastructure of *B. napus* zygotic embryos, characterized, among other features, by a dramatic increase of starch and lipid deposits (Fig. 4D').

All these observations were in perfect agreement with the subcellular architecture widely reported for these stages of *in vivo* microspore development and *in vitro* MDE growth in *B. napus* as well as in many other species. These cells were subjected to the same processing techniques as embryogenic microspores, but no signs of massive excretion or autophagy were observed. Thus, it is concluded that the remarkable differences of embryogenic microspores should not be attributable to artefacts produced by processing techniques, but to a series of real structural and physiological changes.

Autophagosome-like bodies of embryogenic microspores accumulate and excrete MDC-positive bodies

From the work presented above, it appeared that embryogenic microspores produce autophagosomes and lytic vacuoles

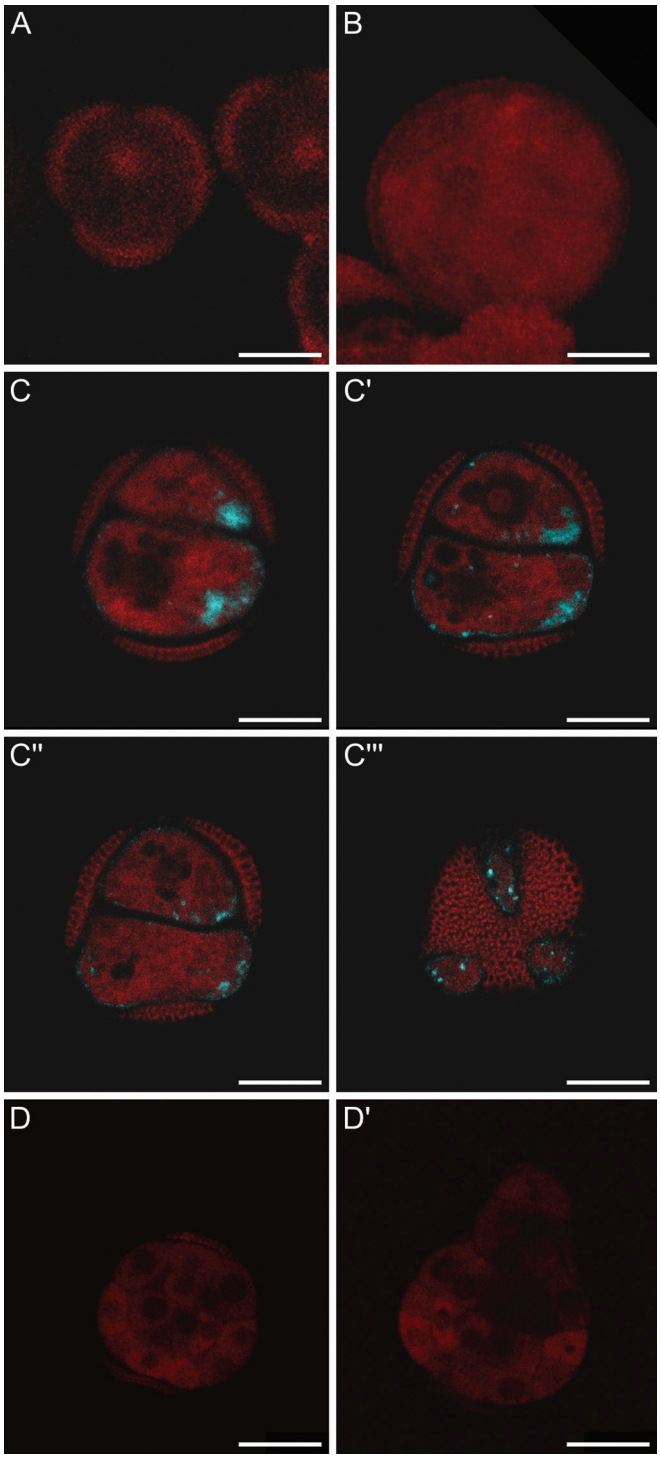

Fig. 5. Confocal images of cultured microspores, microspore-derived structures, and MDEs stained with MDC and PI. Blue signal corresponds to MDC, whereas the red signal corresponds to PI general staining of nuclear and cytoplasmic nucleic acids. (A) Freshly isolated microspore, before application of the inductive treatment. (B) Pollen-like structure. (C–C''') Confocal slices of the same embryogenic microspore. Note that the blue, fluorescent signal of MDC is clearly visible within the cells, but also in the extracytoplasmic space, as revealed by the visibility of blue spots at the apertures, devoid of exine (C'''). (D, D') Confocal slices of the same MDE showing the region of the embryo proper (D) and part of a suspensor (D'). Bars: A–C''', 10 μm; D, D', 20 μm.

whose content, instead of being completely digested and recycled, is excreted out of the cell. Since this is not a commonly accepted mechanism for autophagy, freshly isolated microspores and microspore cultures were incubated with MDC, in order to confirm the observations by a parallel approach. MDC is an autofluorescent amine that specifically stains autophagosomes both in plants (Contento *et al.*, 2005) and in animals (Munafó and Colombo, 2001). To have a reference of the subcellular staining pattern of MDC, cells were also stained with PI. PI is a general stain for nucleic acids, binding both DNA and RNA. Thus, when a previous RNase treatment is omitted, the cytoplasm is also stained with PI (Suzuki *et al.*, 1997). Observation of freshly isolated microspores stained with MDC showed no traces of accumulation of MDC within the microspore (Fig. 5A). In 4-day-old cultures, no MDC signal was observed in pollen-like structures (Fig. 5B). However, this scenario changed when embryogenic microspores were analysed. Figure 5C–C''' corresponds to a series of confocal slices from a representative embryogenic microspore, covering different planes from the equator to the pole. In this series, it is evident that MDC-positive bodies were present in the cytoplasm of these cells, with a size and shape in accordance with the autophagosomes and autophagic vacuoles observed in TEM images. In addition, MDC-positive spots were observed outside the cytoplasm, in the space between the plasma membrane and the microspore coat. This is particularly evident in Fig. 5C''', where the absence of exine in the apertures revealed MDC-positive spots together with the intine. Finally, when small globular MDEs were analysed 4 d after cessation of the induction treatment, MDC fluorescence could not be detected in any cell of either the embryo proper (Fig. 5D) or the suspensor (Fig. 5D'). Based on this evidence, it was concluded that the MDC-positive spots corresponded to the autophagosomes observed in TEM images of HPF/FS-processed samples, and to their cell wall-excreted cargo.

Discussion

Induction of microspore embryogenesis implies a profound cytoplasmic cleaning based on autophagy mechanisms

Two principal autophagic mechanisms have been described to operate in induced microspores. These two mechanisms would be essentially comparable with the known plant microautophagic and macroautophagic pathways (Bassham, 2007; Li and Vierstra, 2012). Direct evidence for the occurrence of such events during microspore embryogenesis is nearly absent to date. In 1974, Sunderland and Dunwell described the lysosome-mediated destruction of some organelles in induced tobacco microspores. Apart from this, other previous observations such as reductions in the number of ribosomes, starch granules, and lipid bodies, and presence of organelle-free regions (reviewed in Maraschin *et al.*, 2005) have been considered as indirect proof for some sort of large-scale cell cleaning. Based on this, several reviews speculated about autophagy as a way to remove gametogenesis-related molecules and stress-damaged cellular components from the cytoplasm of induced microspores (Maraschin *et al.*, 2005; Forster *et al.*, 2007; Hosp *et al.*, 2007). However, to the authors' knowledge, this is the first time that microautophagy and macroautophagy are specifically documented during microspore embryogenesis. With respect to microautophagy, evidence was provided of invaginating membranes in vacuoles containing single membrane-bound autophagic bodies similar to those previously described as produced by microautophagy events (Van der Wilden *et al.*, 1980; Saito *et al.*, 2002). As for macroautophagy, the presence of cup-shaped phagophores engulfing portions of cytoplasm was identified. These structures are necessary intermediates in the process of autophagosome generation (Li and Vierstra, 2012). The massive production of autophagosomes only in the cytoplasm of cells of embryogenic microspores, and not in cells of other structures either before, during, or after the inductive period, was also shown by TEM and confocal imaging. These bodies were double membrane-bound, and remarkably similar in morphology and size to the autophagosomes previously described in other plant cell types (Aubert *et al.*, 1996; Otegui *et al.*, 2005; Lundgren Rose *et al.*, 2006; Reyes *et al.*, 2011). Based on these lines of evidence, it is reasonable to assume that what is being observed are autophagosomes and autophagic vacuoles involved on the massive removal of useless cytoplasmic material. Thus, both microautophagy and macroautophagy would co-exist in embryogenic microspores, although, according to the relative abundance of microautophagic and macroautophagic profiles, macroautophagy would be the preferred pathway for cytoplasm cleaning in *B. napus*-induced microspores.

Plants use two principal ways to recycle/remove useless cell material, the ubiquitin/26S proteasome system (UPS) and autophagy. UPS is principally aimed at the selective removal of small regulatory proteins (Smalle and Vierstra, 2004). In contrast, autophagy is considered as a housekeeping system to remove and recycle rapidly cellular debris including non-proteinaceous material, large particles such as organelles, and even entire cytoplasmic regions, as a response to stress conditions (principally starvation) or during developmental transitions (Bassham, 2009; Liu and Bassham, 2012). Considering that stress-induced, embryogenic microspores undergo dramatic developmental changes while simultaneously exposed to severe abiotic stresses, it could be argued that autophagy might be a consequence of the previous exposure to heat shock during the inductive period. However, it was shown that pollen-like microspores, also exposed to heat stress in the same culture environment, do not present any of the autophagy-related features described here. Thus, cytoplasmic cleaning would be a direct and exclusive consequence of the embryogenic induction. This is in agreement with older studies reporting that organelle-free cytoplasmic regions occurred only in heat-treated, cultured *B. napus* microspores, but not in microspores of heat-treated whole plants (Telmer *et al.*, 1993). It is also consistent with recent reports describing the up-regulation of genes involved in the UPS pathway, exclusively during androgenesis induction (Maraschin *et al.*, 2006). This led the authors to propose an association between the acquisition of androgenic competence and UPS-mediated

protein degradation. In line with this, here an extension of this association no only with proteolysis, but also with autophagy, is proposed which would account for the extensive degradation of cytoplasmic material associated with the androgenic switch.

Excretion of autophagosomal cargo appears essential for proper microspore embryogenesis

Perhaps the most intriguing observation presented in this work relates to the abundant material present between the plasma membrane and the cell wall of embryogenic microspores, and not of microspores before induction, pollen-like structures, non-embryogenic structures, or MDEs. Many autophagosomes and small vacuoles were observed fusing with the plasma membrane, and exposing their luminal contents to the cell wall, where massive amounts of fibrillar and membranous material were identified. In addition, MDC-positive spots were observed not only within the cytoplasm but also outside the cytoplasm, between the plasma membrane and the cell wall, in the same regions where the excreted material is observed in TEM images. This evidence is clearly divergent from the normal dynamics of autophagosomes. Usually, the final fate of plant autophagosomes is to fuse with lytic vacuoles, the major site for the degradation and recycling of autophagosomal cargo (Bassham, 2009). Alternatively, autophagosomes may be functionally self-sufficient to digest their cargo in an autonomous manner, or may also fuse opportunistically to other autophagosomes at different stages of their digestive process (Lundgren Rose *et al.*, 2006). In this work, ultrastructural evidence of the occurrence of these processes in *B. napus* embryogenic microspores was provided (Fig. 6, light grey arrows). Moreover, evidence was also shown to support that at least some of the compartments involved in the lytic pathway (including autophagosomes, small vacuoles, and pre-vacuolar compartments) may be alternatively redirected towards the plasma membrane (Fig. 6, dark grey arrows), thus truncating their conventional dynamics. This alternative pathway would imply that upon membrane fusion, autophagosomes would release their partially degraded cargo, accounting for the abundant presence of fibrillar and membranous material in the cell wall. Then, the question arises as to why autophagosome cargo is not recycled, but is directly excreted out of the cytoplasm.

In the authors' opinion, the most reasonable hypothesis would imply that the cell diverts autophagosomes and pre-vacuolar compartments to fuse with the plasma membrane, in order to prevent excessive growth of the vacuolar system and to ensure a proper embryogenic development (Fig. 7). Fusion of all autophagosomes/pre-vacuolar compartments with lytic vacuoles would lead to the formation of several large vacuoles or one giant, central vacuole like those observed in non-embryogenic structures (Fig. 1D). Vacuoles swell by water uptake, mediated by the osmotic pressure exerted by the osmolytes accumulated. Conventional fusion of all autophagosomes to vacuoles would contribute significant amounts of membrane, and also of different osmolytes, which would cause excessive vacuolar growth and, eventually, cell collapse. Interestingly, very recent time-lapse recordings of the very first moments of the androgenic switch in living barley microspores have shown that whereas some vacuolated microspores enter a programme of rapid divisions and soon become MDEs, other microspores divide just one or few times while their vacuoles grow quickly and massively, inflating the microspores up to a point when they burst, collapse, and die (Dr J. Kumlehn, personal communication).

Alternatively, excessive (but sublethal) vacuolation would arrest embryo growth, as was observed for the non-embryogenic structures of the *B. napus* microspore cultures. Such an arrest could be derived from the alteration of essential processes in this zygote-like cell type, such as the establishment of polarity through auxin gradients, the series of programmed divisions necessary to establish the embryo pattern, the formation of the mitotic spindle for caryokinesis, or the assembly of the large phragmoplast machinery for cytokinesis. In *Arabidopsis* meristem cells, the volume of the interphasic vacuolar system is dramatically reduced to nearly 80% of the initial volume to accommodate the phragmoplast microtubule array and associated cell plate-forming structures (Seguí-Simarro and Staehelin, 2006). Conceivably, keeping a

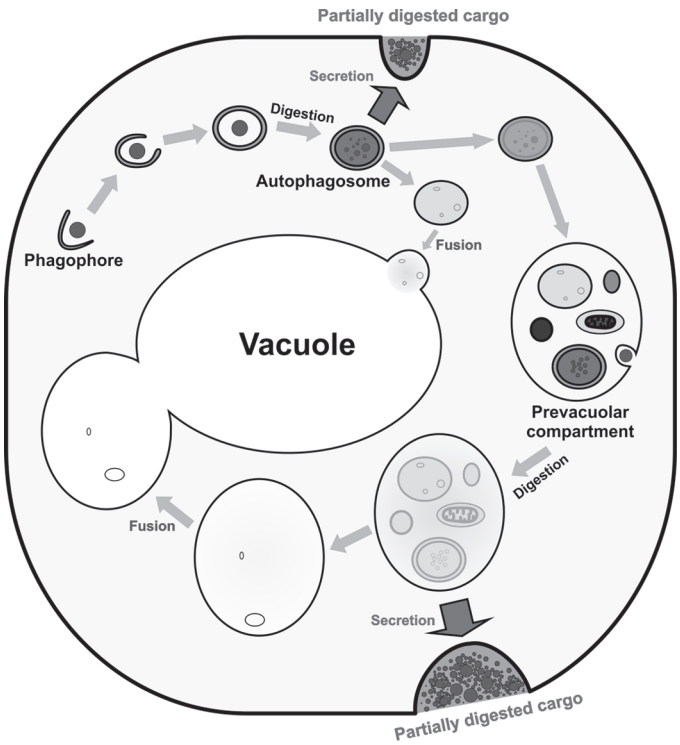

Fig. 6. Proposed model of cytoplasmic cleaning for *B. napus* embryogenic microspores. Cytoplasmic material is engulfed by phagophores and then embedded into autophagosomes. The autophagosomes may follow a conventional lytic pathway (light grey arrows), including digestion of cargo, fusion with lytic vacuoles or with other lytic compartments, and finally recycling of the digested contents. In parallel, autophagosomes are deviated from this pathway and directed to the plasma membrane (dark grey arrows), where they fuse and excrete their partially digested cargo to the cell wall.

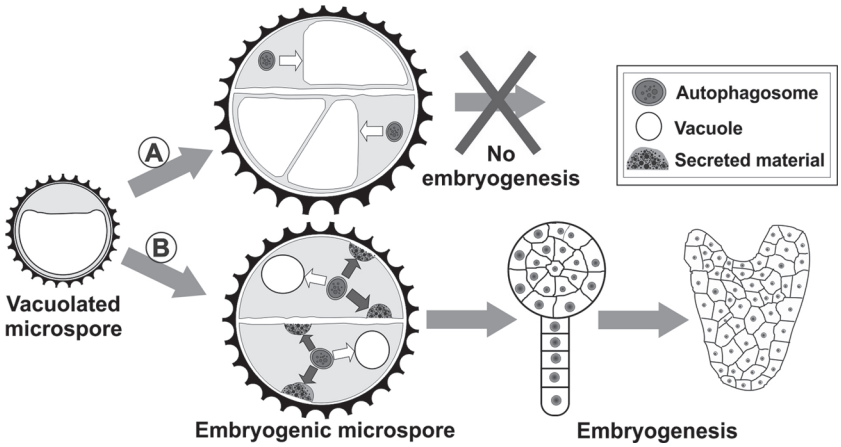

Fig. 7. Proposed relationship of autophagy and excretion to microspore embryogenesis. Vacuolated microspores exposed to the inductive treatment may produce two types of dividing microspores, depending on how they recycle their cytoplasm. Those following the A route produce autophagosomes that follow the conventional lytic pathway (white arrows). This pathway will end up with fusion of vacuoles, digestion, and recycling of the vacuolar content. Such fusion will induce massive vacuolar growth, incompatible with progression of embryogenesis. Those following the B route produce some autophagosomes that follow the conventional lytic pathway (white arrows), and also others that are diverted towards the plasma membrane (dark grey arrows), in order to fuse with it and excrete their cargo to the cell wall. In this way, the cell can retain its proliferative architecture, and progression of embryogenesis can continue.

reduced vacuolar volume must be essential in embryogenic microspores as well. Vacuole swelling would also displace the division plane, giving rise to asymmetric cells, and inducing an undesired increase in cell size. It is known that cell expansion driven by growth of the central vacuole is a clear sign of cell differentiation. This is consistent with the fact that starch deposits (amyloplasts), known markers of pollen differentiation, were frequently observed in non-embryogenic structures (Fig. 1D). Therefore, excretion would be a 'safety system' to prevent vacuolar growth and the subsequent transformation of the cell architecture of embryogenic microspores. Non-excreting cells would recycle their contents and, in parallel, would give rise to large, vacuolated, and differentiated, non-embryogenic structures that will eventually stop their growth and die (Fig. 7).

HPF/FS emerges as the best approach to study the subcellular changes associated with the androgenic switch

The present study is not the first focused on the ultrastructural changes associated with induction of microspore embryogenesis. Indeed, different groups followed this approach during the past and the present century (see Introduction), providing numerous and valuable results that helped im understanding the complexity of this process. However, only few of the results presented in this work have been described before, and in an occasional manner. This is the case of extracytoplasmic vesicles and dense deposits. In *B. napus*, Telmer *et al.* (1993) described that 'cultured embryogenic microspores contained electron-dense deposits at the plasma membrane/cell wall interface, vesicle-like structures in the cell walls and organelle-free regions in the cytoplasm'. In *N. tabacum*, Rashid *et al.* (1982) mentioned the presence of 'electron dense inclusions' in cell walls. Similarly, in *Capsicum annuum* González-Melendi *et al.* (1995) found 'electron opaque deposits in the cytoplasmic vacuoles' that remained after several cell cycle divisions. Telmer *et al.* (1995) showed that the presence of such deposits was reversible, since they were absent in *B. napus* proembryos. However, none of these works provided an explanation for their occurrence, possibly due to the lack of reliable evidence pointing to their excretion from the cytoplasm. Apart from these, to the authors' knowledge there were no other previous mentions of the structures and processes described in this work. So the question arises as to why they have not been consistently reported before in the literature.

In the authors' opinion, the answer to this lies in the methodology used for sample processing. From the pioneering studies to the most recent reports, all of current knowledge of the ultrastructural changes undergone by androgenic microspores is derived from studies of chemically fixed cells. Up to now, HPF/FS methods have never been applied to the study of the androgenic switch. As mentioned in the Introduction, the most limiting aspect of chemical fixatives is their inability to preserve membranous elements in a reliable manner. An illustrative exercise to realize how HPF/FS may improve the preservation of cell membranes can be done by comparing the appearance of the membranous elements shown in this work (Golgi stacks, tonoplast, ER, nuclear envelope, plasma membrane, etc.) with those from the studies mentioned above. Therefore, it is reasonable to think that in previous studies, many of the new structures described here were not observed simply because they were not properly preserved. It is likely that many other membranous structures were previously observed, but, due to the effect of chemical fixatives on membranes, they were not considered as real structures, but as artefacts. Conceivably, these 'artefacts' and the cells containing them would have been just dismissed. This could well be the case for autophagosomes, never reported in TEM studies of embryogenic microspores despite the fact that TEM is

the most reliable method to detect them (Chung, 2011). For example, the works of Dunwell and Sunderland (1975) and Sunderland and Dunwell (1974) in *N. tabacum* embryogenic microspores described the occasional presence of lysosomes, but their pictures also showed extensive vesiculation of the cytoplasm and profiles suggestive of fusion of large vesicles with the plasma membrane. They could well correspond to the different autophagosomes and vacuolar compartments described here. Similar studies in *B. napus* by Telmer *et al.* (1993, 1995) showed many vacuole-like structures, filled with substances of variable electron density, and many of them with membranous and multilamellar remnants, but no specific mention was made of them.

Thus, it can be concluded that the identification of the structures and processes shown in this work has been possible thanks to the use of cutting-edge technologies for ultrastructural preservation such as HPS/FS. These methodologies have been previously applied to the study of natural processes in a broad spectrum of plant tissues, with remarkable success. However, their use in a complex experimental system such as *in vitro* induction of microspore embryogenesis appears especially useful. The results presented here are just an example of their possibilities. Hopefully, they will open the door for further revisions of the ultrastructural changes undergone by the reprogrammed microspore. In parallel, the application of this approach to the study of microspore embryogenesis in recalcitrant species may help to elucidate the cellular basis of such recalcitrance.

Concluding remarks

In this work, a link has been established between autophagy, excretion, cytoplasmic cleaning, and induction of microspore embryogenesis. It appears that for a successful induction, cells must eliminate all the damaged or useless (gametophytic) machinery, either before triggering of the embryogenic programme, or simultaneously as proposed by Malik *et al.* (2007). According to the accepted role of autophagy as a housekeeping process for the breakdown of damaged or unwanted cellular components, the digested and excreted material would include protein aggregates and remnants of incomplete or defective cell plates frequently found in embryogenic microspores. Accordingly, large multilamellar bodies would derive from the digestion of damaged or useless organelles. Alternatively, the excreted material could also include specific proteins and macromolecules initially destined for pollen differentiation, but no longer needed in the new, embryogenic scenario. This would be consistent with the recent view of autophagy as a highly selective process mediated by recruitment proteins that tether specific cargo to the enveloping autophagosomes (Li and Vierstra, 2012). In summary, autophagy and excretion would be essential processes in the transition towards embryogenesis. Future research should focus on the molecular mechanisms by which embryogenic microspores alter their conventional autophagic pathway. In other words, the analysis of the expression of autophagy-related genes (ATG8, etc.) during these stages would surely help to elucidate the molecular basis of this process.

Supplementary data

Supplementary data are available at *JXB* online.

Figure S1. Distribution of diameter frequencies for vesicles of cell wall depositions and for Golgi-derived vesicles.

Acknowledgements

We especially thank Professor L. Andrew Staehelin for his kindness, knowledge, friendship, and help during the stay of JMSS at his lab at the University of Colorado. We also want to express our thanks to Tom Giddings from the MCDB Electron Microscopy Facility, to the staff of the EBIO greenhouses, both at University of Colorado, to the staff of the Electron Microscopy Service of Universitat Politècnica de València, and to Dr Kim Boutilier for her help during the stay of VPV at her lab. This work was supported by the following grants to JMSS: AGL2006-06678 and AGL2010-17895 from the Spanish MICINN, and BEST/2008/154 and ACOMP/2012/168 from Generalitat Valenciana.

References

Aubert S, Gout E, Bligny R, Marty-Mazars D, Barrieu F, Alabouvette J, Marty F, Douce R. 1996. Ultrastructural and biochemical characterization of autophagy in higher plant cells subjected to carbon deprivation: control by the supply of mitochondria with respiratory substrates. *Journal of Cell Biology* **133,** 1251–1263.

Bassham DC. 2007. Plant autophagy—more than a starvation response. *Current Opinion in Plant Biology* **10,** 587–593.

Bassham DC. 2009. Function and regulation of macroautophagy in plants. *Biochimica et Biophysica Acta* **1793,** 1397–1403.

Chung T. 2011. See how I eat my greens—autophagy in plant cells. *Journal of Plant Biology* **54,** 339–350.

Contento AL, Xiong Y, Bassham DC. 2005. Visualization of autophagy in Arabidopsis using the fluorescent dye monodansylcadaverine and a GFP–AtATG8e fusion protein. *The Plant Journal* **42,** 598–608.

Dunwell JM. 2010. Haploids in flowering plants: origins and exploitation. *Plant Biotechnology Journal* **8,** 377–424.

Dunwell JM, Sunderland N. 1974a. Pollen ultrastructure in anther cultures of *Nicotiana tabacum* I. Early stages of culture. *Journal of Experimental Botany* **25,** 352–361.

Dunwell JM, Sunderland N. 1974b. Pollen ultrastructure in anther cultures of *Nicotiana tabacum* II. Changes associated with embryogenesis. *Journal of Experimental Botany* **25,** 363–373.

Dunwell JM, Sunderland N. 1975. Pollen ultrastructure in anther cultures of *Nicotiana tabacum* III. The first sporophytic divisions. *Journal of Experimental Botany* **26,** 240–252.

Dunwell JM, Sunderland N. 1976a. Pollen ultrastructure in anther cultures of *Datura innoxia*. I. Division of the presumptive vegetative cell. *Journal of Cell Science* **22,** 469–480.

Dunwell JM, Sunderland N. 1976b. Pollen ultrastructure in anther cultures of *Datura innoxia*. II. The generative cell wall. *Journal of Cell Science* **22,** 481–491.

Dunwell JM, Sunderland N. 1976c. Pollen ultrastructure in anther cultures of *Datura innoxia*. III. Incomplete microspore division. *Journal of Cell Science* **22,** 493–501.

Forster BP, Heberle-Bors E, Kasha KJ, Touraev A. 2007. The resurgence of haploids in higher plants. *Trends in Plant Science* **12,** 368–375.

Germanà MA. 2011. Anther culture for haploid and doubled haploid production. *Plant Cell, Tissue and Organ Culture* **104,** 283–300.

Gilkey JC, Staehelin LA. 1986. Advances in ultrarapid freezing for the preservation of cellular ultrastructure. *Journal of Electron Microscopy Technique* **3,** 177–210.

González-Melendi P, Testillano PS, Ahmadian P, Fadón B, Vicente O, Risueño MC. 1995. *In situ* characterization of the late vacuolate microspore as a convenient stage to induce embryogenesis in *Capsicum*. *Protoplasma* **187,** 60–71.

Hause G, Hause B, van Lammeren AAM. 1992. Microtubular and actin filament configurations during microspore and pollen development in *Brassica napus* cv. Topas. *Canadian Journal of Botany* **70,** 1369–1376.

Hosp J, Maraschin SDF, Touraev A, Boutilier K. 2007. Functional genomics of microspore embryogenesis. *Euphytica* **158,** 275–285.

Kasha KJ. 2005. Chromosome doubling and recovery of doubled haploid plants. In: Palmer CE, Keller WA, Kasha KJ, eds. *Haploids in crop improvement II* , Vol. **56**. Berlin: Springer-Verlag, 123–152.

Lee RMKW, McKenzie R, Kobayashi K, Garfield RE, Forrest JB, Daniel EE. 1982. Effects of glutaraldehyde osmolarities on smooth muscle cell volume, and osmotic reactivity of the cells after fixation. *Journal of Microscopy* **125,** 77–88.

Li F, Vierstra RD. 2012. Autophagy: a multifaceted intracellular system for bulk and selective recycling. *Trends in Plant Science* **17,** 526–537.

Lichter R. 1982. Induction of haploid plants from isolated pollen of *Brassica napus*. *Zeitschrift fur Pflanzenphysiologie* **105,** 427–434.

Liu Y, Bassham DC. 2012. Autophagy: pathways for self-eating in plant cells. *Annual Review of Plant Biology* **63,** 215–237.

Lundgren Rose T, Bonneau L, Der C, Marty-Mazars D, Marty F. 2006. Starvation-induced expression of autophagy-related genes in Arabidopsis. *Biology of the Cell* **98,** 53–67.

Malik MR, Wang F, Dirpaul JM, Zhou N, Polowick PL, Ferrie AMR, Krochko JE. 2007. Transcript profiling and identification of molecular markers for early microspore embryogenesis in *Brassica napus*. *Plant Physiology* **144,** 134–154.

Maraschin SDF, Caspers M, Potokina E, Wulfert F, Graner A, Spaink HP, Wang M. 2006. cDNA array analysis of stress-induced gene expression in barley androgenesis. *Physiologia Plantarum* **127,** 535–550.

Maraschin SF, de Priester W, Spaink HP, Wang M. 2005. Androgenic switch: an example of plant embryogenesis from the male gametophyte perspective. *Journal of Experimental Botany* **56,** 1711–1726.

Munafó DB, Colombo MI. 2001. A novel assay to study autophagy: regulation of autophagosome vacuole size by amino acid deprivation. *Journal of Cell Science* **114,** 3619–3629.

Otegui MS, Noh YS, Martinez DE, Vila Petroff MG, Staehelin LA, Amasino RM, Guiamet JJ. 2005. Senescence-associated vacuoles with intense proteolytic activity develop in leaves of Arabidopsis and soybean. *The Plant Journal* **41,** 831–844.

Pauls KP, Chan J, Woronuk G, Schulze D, Brazolot J. 2006. When microspores decide to become embryos—cellular and molecular changes. *Canadian Journal of Botany-Revue Canadienne de Botanique* **84,** 668–678.

Rashid A, Siddiqui AW, Reinert J. 1982. Subcellular aspects of origin and structure of pollen embryos of *Nicotiana*. *Protoplasma* **113,** 202–208.

Reyes FC, Chung T, Holding D, Jung R, Vierstra R, Otegui MS. 2011. Delivery of prolamins to the protein storage vacuole in maize aleurone cells. *The Plant Cell* **23,** 769–784.

Saito C, Ueda T, Abe H, Wada Y, Kuroiwa T, Hisada A, Furuya M, Nakano A. 2002. A complex and mobile structure forms a distinct subregion within the continuous vacuolar membrane in young cotyledons of Arabidopsis. *The Plant Journal* **29,** 245–255.

Seguí-Simarro JM. 2010. Androgenesis revisited. *Botanical Review* **76,** 377–404.

Seguí-Simarro JM, Nuez F. 2008a. How microspores transform into haploid embryos: changes associated with embryogenesis induction and microspore-derived embryogenesis. *Physiologia Plantarum* **134,** 1–12.

Seguí-Simarro JM, Nuez F. 2008b. Pathways to doubled haploidy: chromosome doubling during androgenesis. *Cytogenetic and Genome Research* **120,** 358–369.

Seguí-Simarro JM, Otegui MS, Austin JR, Staehelin LA. 2008. Plant cytokinesis—insights gained from electron tomography studies. In: Verma DPS, Hong Z, eds. *Cell division control in plants* , Vol. **9**. Berlin: Springer, 251–287.

Seguí-Simarro JM, Staehelin LA. 2006. Cell cycle-dependent changes in Golgi stacks, vacuoles, clathrin-coated vesicles and multivesicular bodies in meristematic cells of Arabidopsis thaliana: a quantitative and spatial analysis. *Planta* **223,** 223–236.

Seguí-Simarro JM, Testillano PS, Risueño MC. 2003. Hsp70 and Hsp90 change their expression and subcellular localization after microspore embryogenesis induction in *Brassica napus* L. cv Topas. *Journal of Structural Biology* **142,** 379–391.

Shariatpanahi ME, Bal U, Heberle-Bors E, Touraev A. 2006. Stresses applied for the re-programming of plant microspores towards *in vitro* embryogenesis. *Physiologia Plantarum* **127,** 519–534.

Simmonds DH, Keller WA. 1999. Significance of preprophase bands of microtubules in the induction of microspore embryogenesis of *Brassica napus*. *Planta* **208,** 383–391.

Smalle J, Vierstra RD. 2004. The ubiquitin 26S proteasome proteolytic pathway. *Annual Review of Plant Biology* **55,** 555–590.

Sunderland N, Dunwell JM. 1974. Anther and pollen culture. In: Street HE, ed. *Plant tissue and cell culture* . Oxford: Blackwell Scientific Publications, 223–265.

Suzuki T, Fujikura K, Higashiyama T, Takata K. 1997. DNA staining for fluorescence and laser confocal microscopy. *Journal of Histochemistry and Cytochemistry* **45,** 49–53.

Telmer CA, Newcomb W, Simmonds DH. 1993. Microspore development in *Brassica napus* and the effect of high temperature on division *in vivo* and *in vitro*. *Protoplasma* **172,** 154–165.

Telmer CA, Newcomb W, Simmonds DH. 1995. Cellular changes during heat shock induction and embryo development of cultured microspores of *Brassica napus* cv. Topas. *Protoplasma* **185,** 106–112.

Testillano PS, Coronado MJ, Seguí-Simarro JM, Domenech J, Gonzalez-Melendi P, Raska I, Risueño MC. 2000. Defined nuclear changes accompany the reprogramming of the microspore to embryogenesis. *Journal of Structural Biology* **129,** 223–232.

Van der Wilden W, Herman EM, Chrispeels MJ. 1980. Protein bodies of mung bean cotyledons as autophagic organelles. *Proceedings of the National Academy of Sciences, USA* **77,** 428–432.

Wu HJ, Liu XH, Chen K, Cai ZP, Luo XJ, Zhang T, Wang XY. 2009. Disintegration of microsporocytes in a male sterile mutant of *Brassica napus* L. is possibly associated with endoplasmic reticulum-dependent autophagic programmed cell death. *Euphytica* **170,** 263–274.

Zaki MA, Dickinson HG. 1990. Structural changes during the first divisions of embryos resulting from anther and free microspore culture in *Brassica napus*. *Protoplasma* **156,** 149–162.

Zaki MAM, Dickinson HG. 1991. Microspore-derived embryos in *Brassica*: the significance of division symmetry in pollen mitosis I to embryogenic development. *Sexual Plant Reproduction* **4,** 48–55.